Preprints.org

Article

Effect of road marking materials on LiDAR response

Yongqi Zhao [*] , Hexuan Li , Philipp Rosenberger , Dario Babić , Darko Babić , Friedrich Wiesinger , Bernhard Helmreich , Tomasz Burghardt , Arno Eichberger

Article

Effect of Road Marking Materials on LiDAR Response

Yongqi Zhao [1],[*] , **Hexuan Li [1]** , **Philipp Rosenberger [2]** , **Dario Babić [3]** , **Darko Babić [3]** ,
Friedrich Wiesinger [4] , **Bernhard Helmreich [4]** , **Tomasz E. Burghardt [4]** and **Arno Eichberger [1]**

[1] Institute of Automotive Engineering, Graz University of Technology, 8010 Graz, Austria;
    yongqi.zhao@tugraz.at, hexuan.li@tugraz.at, arno.eichberger@tugraz.at
[2] Persival GmbH, 64372 Ober-Ramstadt, Germany; philipp.rosenberger@persival.de
[3] University of Zagreb, Faculty of Transport and Traffic Sciences, 10000 Zagreb, Croatia; dbabic2@fpz.unizg.hr,
    dbabic@fpz.unizg.hr
[4] M. Swarovski GmbH, 3363 Neufurth, Austria; friedrich.wiesinger@swarco.com,
    bernhard.helmreich@swarco.com, tomasz.burghardt@swarco.com
*   Correspondence: yongqi.zhao@tugraz.at

Abstract: Road marking recognition is of great importance for the deployment of automated driving systems and for already existing driver line-keeping assistance systems. For proper and reliable function of machine vision systems that include LiDAR and camera, road markings must be visible to them to facilitate planning of driving trajectory. In this study, LiDAR intensity and the number of LiDAR points collected from a field analysis of two road markings systems reflectorised with premium and standard glass beads were analysed. In the lateral direction, it was demonstrated that the use of premium glass beads for road markings lead to 56% higher LiDAR intensity and 14% more LiDAR points captured than in case of standard road markings. In the longitudinal direction, premium road markings showed less distance attenuation, which is seen as advantageous for trajectory planning by machine version systems. The outcomes of this study offer insights for road infrastructure decision-makers, developers of automated driving systems, and researchers in the field of transportation technology.

Keywords: laser intensity; glass beads; automated driving system; retroreflection

1. Introduction

In recent years, Automated Driving Systems (ADS) have gained increased attention as a way of improving the driving experience. The trajectory planning done by the ADS mostly relies on input from sensors such as Light Detection and Ranging (LiDAR) and cameras [1–3]. Unlike cameras that can be blinded by glare, LiDAR is not sensitive to external lighting; thus it plays a profound role in ADS. The robustness of LiDAR-based Road Markings (RM) recognition can be affected by the selection of glass beads (GB) used to reflectorise them [4]; specifically, Refractive Index (RI) of the GB, which directly influences the retroreflectivity of the road markings, holds particular significance. It must be understood that all RM are reflectorised with GB, which provide retroreflectivity (a phenomenon of reflecting back toward the driver the light from vehicle's headlights); in case of LiDAR, the same phenomenon affects the intensity response. It has been reported that the type of RM is essentially irrelevant for LiDAR response, given equal retroreflectivity [5].

Even though the significance of RM for the development of ADS has been proven, nearly all previous studies merely focus on the process of their recognition without paying much attention to the RM themselves [6,7]; only recently the effect of different materials used for RM on their perception by ADS equipment has been studied [4,5,8]. Firstly, the importance of GB selection for enhancing retroreflectivity of RM was interpreted [4]. Subsequently, eight types of RM reflectorised with various GB were tested in the biggest climatic wind tunnel in the world for the recognition by LiDAR and camera with quantifying the influence of adverse weather [5]. In the latest investigation [8], the

recognition of two types of RM by LiDAR and camera was assessed, revealing the necessity to employ structured materials capable of water drainage for reliable detection.

The aforementioned studies shed light on the feasibility of improving RM for more reliable recognition by LiDAR and cameras, yet these investigations were conducted indoors or using static tests, which deviated from the real driving conditions. Therefore, to validate the results, dynamic testing, with readings obtained from LiDAR mounted on a moving vehicle was done. The analysed RM comprised flat lines reflectorised with GB characterised by RI 1.5 (standard materials) and structured markings reflectorised with GB having RI 1.6–1.7 (premium materials); these are known in the industry to represent the two extreme cases in terms of visibility and durability. The assessment included not only comparison of the materials, but also the effect of the distance between the LiDAR sensor and the analysed RM, which appears to be an unexplored research topic. The results could help in identification of the most sustainable RM from the perspective of detection reliability. The outcome was also envisaged as a support for engineers developing the detection algorithms and for road administrators searching for the optimum solutions to maintain the infrastructure so it could be compatible with ADS, as was recently mandated [9].

2. Methodology

2.1. Road marking

The specificity of RM – a unique double layer industrial coating system comprising the bottom paint layer and the top drop-on GB layer - has to be emphasized [10]. While the paint furnishes colour contrasting with the roadway surface, the GB provide retroreflection that is enhancing visibility at night on unlit roads and simultaneously plays a profound role in protecting the paint layer from abrasion [11]. Retroreflectivity is the key parameter of RM used to determine their functional service life. Per standard EN 1436 [12], retroreflectivity is measured as coefficient of retroreflected luminance (R_L) and expressed in $mcd/m^2/lx$.

The evaluated RM and their properties are described in Table 1; the main difference was the selection of drop-on GB, which provided dissimilar R_L and as such should result in different LiDAR response. The materials were procured commercially and applied by professional industrial application crew. Both static and dynamic methods for measuring of R_L were utilised [13]; this was done not only to validate the measurement test methods, but also because the dynamic method was seen as more appropriate for a driving experiment. Small differences in GB diameters were considered, based on professional experience, irrelevant for the purpose of this experiment. External appearance of the evaluated RM is depicted in Figure 1.

Table 1. Evaluated road marking systems.

Road marking type	Standard	Premium
Appearance	Flat lines	Structured lines, random structure
GB type	Standard, RI 1.5	Premium, RI 1.6–1.7
GB diameter range [mm]	0.20–0.80	0.30–0.85
GB drop-on quantity	$0.4\pm0.05\,kg/m^2$	$0.4\pm0.05\,kg/m^2$
Daytime visibility (Qd) [$mcd/m^2/lx$]	192 (14)	141 (13)
R_L [$mcd/m^2/lx$] - dynamic measurements	201 (25)	749 (14)
R_L range [$mcd/m^2/lx$] - dynamic measurements	82–205	92–768
R_L [$mcd/m^2/lx$] - static measurements	236 (29)	708 (64)

*Standard deviations given in parentheses.
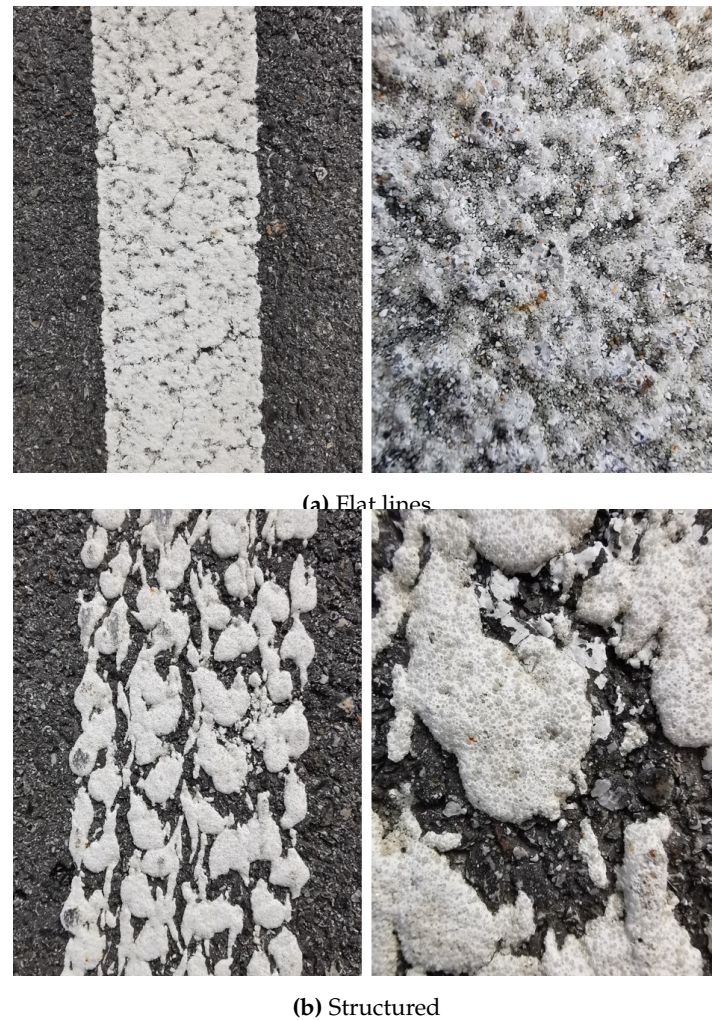
(a) Flat lines

(b) Structured

Figure 1. Appearance of evaluated RM.

2.2. Test site

The evaluation was done at a closed course proving ground located in St. Valentin, Austria. The assessment was done on a road section delimited with three stripes (each 6.0 m long and 0.12 m wide, 12 m apart); the stripes on the left were marked with premium RM and on the right with the standard RM that were described in Table 1. The small sample size was deemed sufficient for reliable results; indeed even smaller sample sizes are required to obtain official homologation of RM in Austria [14].

During the measurement collection, another front vehicle was driving in the same lane as the test vehicle. With varying velocities of the front vehicle, the real driving situation was replicated. Data was collected from 25 drives through the test location at speeds 30–60 $\mathrm{km\,h^{-1}}$; there was no precipitation and the road surface was dry. All of the output was merged for the presented analysis.

2.3. LiDAR

LiDAR emits its own laser pulses and measures the time taken for the reflected light to return. The pulse intensity and directionality directly contribute to its capability to operate without being affected by external lighting conditions. Hence, night-time measurements were not included due to predictable similarity with daytime results. This independence from external lighting is amongst the most important advantages of LiDAR; it guarantees accurate and reliable data acquisition even in the presence of glare, which was reported to bring the visibility by camera (and thus by human drivers) to nil [8,15].

The analysis was done with a LiDAR designed for delivering of the environmental perception for ADS. The used 128-beam LiDAR was operating at 950 nm, transmitting power 90 W, with 360° horizontal and $-25°-+15°$ vertical field of view, providing readings within the range 0.4–250 m and capable of delivering distance readings with 3 cm accuracy. The beam widths were 1.5 mrad in horizontal and 3.6 mrad in vertical dimension. It was positioned at the height of 1.8 m above the ground.

Output data included the relative position and intensity of LiDAR point cloud as well as the sensing equipment position. In terms of intensity, the LiDAR manufacturer defined it as a scale to evaluate the ability of the obstacle to reflect light. Instead of reporting the actual strength of returned laser beam, software of the tested equipment provided intensity values varying from 0 to 255, with 0 being the weakest intensity from a black, diffuse reflector and 255 representing the intensity of an ideal reflector. Therefore, for simplicity and easier data presentation, the LiDAR intensity output values of 0–255 were divided by 255 to provide the results in percentages.

2.4. Detection algorithm and data processing

In the data post-processing phase, a detection algorithm based on the prior studies was used [16,17]. The algorithm is composed of three phases: data preprocessing, RM line position detection, and RM line LiDAR points acquisition. During the first phase, LiDAR points reflected from the ground plane were obtained by defining the Region Of Interest (ROI). In the second phase, the acquired LiDAR points were divided into several bins along the lateral direction of the test vehicle. Then, the confidence score of each bin was computed by an equal-weighted sum of intensities and the number of LiDAR points. Subsequently, the histogram of the confidence scores was visualized, where the confidence scores of the RM line positions appear as two peaks, representing the right and the left lines delimiting the traffic lane. Finally, LiDAR points detected from the RM were extracted in the RM line positions based on a predefined intensity threshold, so the RM (the ROI) could be differentiated from the background (the roadway surface). It should be noted that LiDAR points of gaps between RM were not analysed; they were excluded through the use of distance and intensity thresholds.

2.5. Data presentation

The experimental findings were elucidated across three primary aspects. Firstly, the detectability of the tested RM by LiDAR point cloud intensities was examined. The effects of both lateral and longitudinal distance was assessed. In the scatter plots, the intensity values of LiDAR points were depicted, showing their distribution across the measured area. In the boxplots, LiDAR response was illustrated by emphasizing the first quartile, median, and third quartile. All of the results were checked for statistical significance within 95% confidence level using Student's t-test (unpaired, two-tailed distribution); p-values are provided [18].

3. Results

3.1. Lateral position

In Figure 2, a comparison is shown between LiDAR response to the premium and the standard RM along the lateral direction. The intensity peaks correspond to the position of RM. The measured median intensity for premium RM (0.37) was 56% higher than measured for standard RM (0.24). This was expected given the dissimilar R_L of these RM Table 1. The differences were statistically significant with p-value < 0.001.
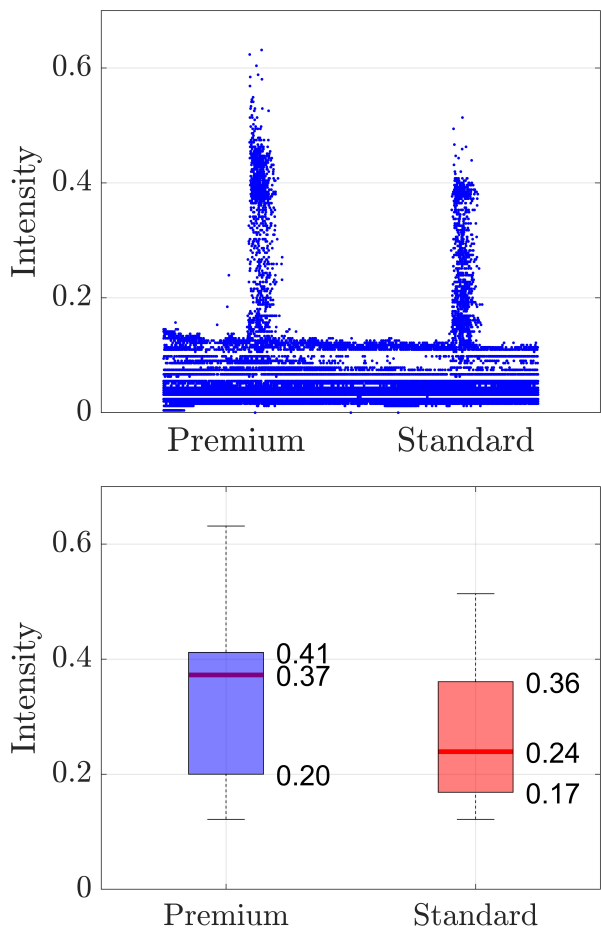
Figure 2. Comparative analysis of LiDAR intensity for premium and standard RM in the lateral direction.

3.2. Longitudinal position

In Figure 3, a comparative analysis of LiDAR response to premium and standard RM along the longitudinal direction is presented. The superior reflective characteristic of premium RM was observed at all sampled distances. In the longitudinal direction, LiDAR intensities from premium RM were 53% (0–15 m), 72% (15–30 m), and 98% (30–45 m) higher than obtained from standard RM.

Very importantly, in case of intensity attenuation over distance, premium RM meaningfully outperformed standard RM. When compared to the range interval 0–15 m, in range intervals 15–30 m and 30–45 m, the intensities from premium RM decreased by 4% and 14% respectively. In contrast, distance attenuation measured with the standard RM was correspondingly 15% and 34%.

In Table 2 is presented intensity attenuation comparison between premium and standard RM over distance. Premium RM consistently exhibited higher intensity levels than standard RM across all range intervals. The median loss of intensity between the shortest and largest distance was only 13% for premium RM, as compared to 36% for the standard RM. Statistical analysis, with p-values shown in Table 2, confirmed the differences.
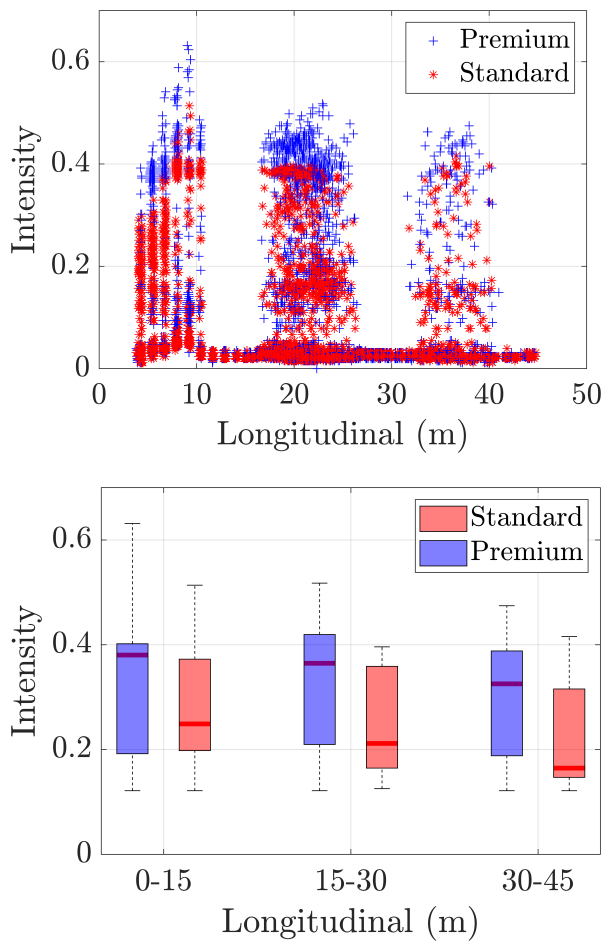
Figure 3. Comparative analysis of LiDAR intensity for premium and standard RM in longitudinal directions.

Table 2. LiDAR intensity in longitudinal direction.

	0–15 m	15–30 m	30–40 m	p-value 0–15 m vs. 15–30 m	p-value 0–15 m vs. 30–45 m
Premium	0.38 (0.19–0.40)	0.36 (0.21–0.42)	0.33 (0.19–0.39)	0.428	0.028
Standard	0.25 (0.20–0.37)	0.21 (0.16–0.36)	0.16 (0.15–0.32)	0.016	< 0.001
p-value	< 0.001	< 0.001	< 0.001	-	-

* Median values are given; ranges in parentheses correspond to the first and third quartile.

3.3. Number of points

A comparison of the number of LiDAR points detected from premium and standard RM of 25 drives in the lateral and longitudinal directions is shown in Table 3. In the lateral direction, the equipment response to premium RM was higher than to standard RM, which is quite puzzling. The same trends were also observed at the range interval 15–45 m. Normally, there should be equal number of points for both as the number and concentration of reflecting elements (glass beads) ought to be similar. Hence, the situation 0–15 m is normal. The number of detected points from both types of RM showed decreasing trends, which, as expected, became more significant with increasing distance.

Table 3. Comparison of the number of LiDAR points in lateral and longitudinal direction.

	Lateral	0–15 m	15–30 m	30–45 m	p-value 0–15 m vs. 15–30 m	p-value 0–15 m vs. 30–45 m
Premium	80 (74–90)	31 (22–40)	43 (37–44)	9 (7–11)	0.002	< 0.001
Standard	70 (63–76)	30 (29–32)	33 (27–37)	6 (5–7)	0.729	< 0.001
p-value	< 0.001	0.734	< 0.001	< 0.001	-	-

* Median values are given; ranges in parentheses correspond to the first and third quartile.

4. Discussion

The outcome of this study is in line with the expectations [8]; the use of RM with higher R_L lead to significantly enhanced LiDAR response in terms of intensity. Very importantly, the use of premium RM resulted in significantly lesser attenuation with increased distance, which should be very advantageous for machine vision algorithms that demand extended look-ahead for reliable trajectory planning. No prior reports related to this aspect were found.

Contrary to previous report [8], the number of detected points was also higher for premium RM. While at present no fully tenable explanation can be provided, it could be theorised that higher vertical positioning of the LiDAR sensor (1.8 m above ground as compared to 0.6 m in previous study), played a role. Positioning of the LiDAR closer to the ground could have resulted in sheltering some of the GB in premium RM (which were in form of a structure up to 4 mm high) from the laser pulses, which would result in lower number of response points reported previously. This issue requires additional investigation.

ADS must demonstrate exceptional reliability prior to deployment [19]. An important aspect influencing their reliability is the visibility of RM. The introduction of high-end, premium RM may improve the reliability of ADS by facilitating the recognition of the traffic lanes and thus improving trajectory planning through providing longer preview distance. The reported increased intensity response of LiDAR to premium RM was possible because they were reflectorised with "premium" GB characterised by higher RI than were used in standard RM.

The use of such GB was also reported as contributing to durability and sustainability of RM. The premium RM were reported as providing longer functional service life than standard RM, which means that they furnished higher R_L over a longer period [20]; as such they would remain more visible to LiDAR. In addition, the use of premium, durable RM could reduce the maintenance cost from the long-term perspective despite higher initial investment [21].

Certain limitations and uncertainties of this study must be acknowledged. Firstly, a RM detection algorithm with empirical threshold values to extract RM LiDAR points was used, which potentially could lead to the inclusion of points not associated with RM and the omission of some points belonging to the RM. Secondly, this experiment was designed to simulate genuine driving situation in Austria; however, it constrained the consideration of other traffic participants and their influence, involving interaction solely with one target vehicle and the ego vehicle.

Amongst identified research needs, one should foremost note that other colours (particularly orange and yellow, which are utilised for temporary RM) should also be tested with the types of GB employed for this study. The effect of GB with RI 1.9 also ought to be evaluated. Testing under other conditions, particularly during rain and snow, has to be done as well; it is worth noting that previous research [5] indicated that better visibility of RM for LiDAR could be correlated with the presence of both structures and GB with increased RI. Confirmation under field conditions would be valuable. Even though this research was done with only one LiDAR, alternate equipment should also be tested.

5. Conclusions

When conventional studies primarily focused on optimizing machine vision perception algorithm; in this research, the topic was addressed from the perspective of materials. The role of "premium" GB, capable of providing higher R_L, was examined; it was shown that their use would be advantageous for

LiDAR sensor. In the course of this study, the response of an automotive LiDAR to two types of RM, varying in R_L, was examined under dry conditions. It was shown that premium RM, reflectorised with GB having RI 1.6–1.7, and furnishing $R_L > 700$ mcd/m^2/lx consistently provided higher intensity than standard RM where GB characterised by RI 1.5 were used and R_L was < 250 mcd/m^2/lx. In addition, there was much lesser distance attenuation when premium RM were utilised, which would permit for more reliable trajectory planning by ADS. Higher R_L should also lead to improvement of road safety through enhancing RM visibility also for human drivers. The presented outcome holds significance for road infrastructure planners and road administrators. As LiDAR technology continues to gain importance in machine vision technologies; the insight from this study offer valuable guidance for the selection and deployment of RM that improve LiDAR sensing capabilities.

Author Contributions: Conceptualization, Y.Z., H.L., A.E.; methodology, Y.Z., H.L, Dario Babić, T.B., P.R., and A.E.; software, Y.Z.; validation, Y.Z.; formal analysis, Y.Z.; investigation, Y.Z.; resources, A.E. and H.L; data curation, Y.Z.; writing—original draft preparation, Y.Z., H.L; writing—review and editing, Dario Babić, Darko Babić, P.R., T.B. and A.E; visualization, Y.Z.; supervision, P.R., T.B. and A.E.; project administration, A.E., F.W., B.H., and T.B.; funding acquisition, A.E. All authors have read and agreed to the published version of the manuscript.

References

1.   Bai, M.; Mattyus, G.; Homayounfar, N.; Wang, S.; Lakshmikanth, S.K.; Urtasun, R. Deep multi-sensor lane detection. 2018 IEEE/RSJ International Conference on Intelligent Robots and Systems (IROS). IEEE, 2018. doi:10.1109/iros.2018.8594388.

2.   Marti, E.; De Miguel, M.A.; Garcia, F.; Perez, J. A review of sensor technologies for perception in automated driving. *IEEE Intelligent Transportation Systems Magazine* **2019**, *11*, 94–108. doi:10.1109/MITS.2019.2907630.

3.   Deilamsalehy, H.; Havens, T.C. Sensor fused three-dimensional localization using IMU, camera and LiDAR. 2016 IEEE Sensors. IEEE, 2016. doi:10.1109/icsens.2016.7808523.

4.   Burghardt, T.E.; Mosböck, H.; Pashkevich, A.; Fiolić, M. Horizontal road markings for human and machine vision. *Transportation Research Procedia* **2020**, *48*, 3622–3633. doi:10.1016/j. trpro.2020.08.089.

5.   Burghardt, T.E.; Popp, R.; Helmreich, B.; Reiter, T.; Böhm, G.; Pitterle, G.; Artmann, M. Visibility of various road markings for machine vision. *Case Studies in Construction Materials* **2021**, *15*, e00579. doi:10.1016/j. cscm.2021.e00579.

6.   Kunze, L.; Bruls, T.; Suleymanov, T.; Newman, P. Reading between the lanes: Road layout reconstruction from partially segmented scenes. 2018 21st International Conference on Intelligent Transportation Systems (ITSC). IEEE, 2018, pp. 401–408. doi:10.1109/itsc.2018.8569270.

7.   Mihalj, T.; Li, H.; Babić, D.; Lex, C.; Jeudy, M.; Zovak, G.; Babić, D.; Eichberger, A. Road infrastructure challenges faced by automated driving: a review. *Applied Sciences* **2022**, *12*, 3477. doi:10.3390/app12073477.

8.   Burghardt, T.E.; Chistov, O.; Reiter, T.; Popp, R.; Helmreich, B.; Wiesinger, F. Visibility of flat line and structured road markings for machine vision. *Case Studies in Construction Materials* **2023**, *18*, e02048. doi:10.1016/j. cscm.2023.e02048.

9.   Directive (EU) 2019/1936 of the European Parliament and of the Council of 23 October 2019 amending Directive 2008/96/EC on road infrastructure safety management. Technical report, European Union, 2019, L 305/1.

10.   Babić, D.; E. Burghardt, T.; Babić, D. Application and characteristics of waterborne road marking paint. *International Journal for Traffic and Transport Engineering* **2015**, *5*, 150–169. doi:10.7708/ijtte.2015.5(2).06.

11.   Burghardt, T.E.; Pashkevich, A. Road markings and microplastics – A critical literature review. *Transportation Research Part D: Transport and Environment* **2023**, *119*, 103740. doi:10.1016/j. trd.2023.103740.

12.   European Standard EN 1436. Road marking materials — road marking performance for road users and test methods. European Committee for Standardization: Brussels, Belgium, 2018.

13. Babić, D.; Fiolić, M.; Žilioniene, D. Evaluation of static and dynamic method for measuring retroreflection of road markings. *Građevinar* **2017**, *69*, 907–914. doi:10.14256/JCE.2010.2017.

14. Standard ONR 22440-1: Bodenmarkierungen. Funktionsdauer Teil 1: Allgemeines. Technical report, Austrian Standards Institute, Wien, Austria, 2018.

15. Li, Y.; Ibanez-Guzman, J. Lidar for autonomous driving: the principles, challenges, and trends for automotive lidar and perception systems. *IEEE Signal Processing Magazine* **2020**, *37*, 50–61. doi:10.1109/MSP.2020.2973615.

16. Ghallabi, F.; Nashashibi, F.; El-Haj-Shhade, G.; Mittet, M.A. LIDAR-based lane marking detection for vehicle positioning in an HD map. 2018 21st International Conference on Intelligent Transportation Systems (ITSC). IEEE, 2018. doi:10.1109/itsc.2018.8569951.

17. Thuy, M.; León, F. Lane detection and tracking based on Lidar data. *Metrology and Measurement Systems* **2010**, *17*. doi:10.2478/v10178-010-0027-3.

18. Hubert, M.; Vandervieren, E. An adjusted boxplot for skewed distributions. *Computational Statistics & Data Analysis* **2008**, *52*, 5186–5201. doi:10.1016/j.csda.2007.11.008.

19. Becker, F.; Axhausen, K.W. Literature review on surveys investigating the acceptance of automated vehicles. *Transportation* **2017**, *44*, 1293–1306. doi:10.1007/s11116-017-9808-9.

20. Burghardt, T.E.; Babić, D.; Pashkevich, A. Sustainability of thin layer road markings based on their service life. *Transportation Research Part D: Transport and Environment* **2022**, *109*, 103339. doi:10.1016/j. trd.2022.103339.

21. Burghardt, T.E.; Pashkevich, A. Materials selection for structured horizontal road markings: financial and environmental case studies. *European Transport Research Review* **2020**, *12*, 11. doi:10.1186/s12544-020-0397-x.